ELSEVIER

Journal of Photochemistry and Photobiology A: Chemistry 109 (1997) 165–170

Journal of PHOTOCHEMISTRY AND PHOTOBIOLOGY A: CHEMISTRY

Photoelectrochemical decomposition of amino acids on a TiO_2/OTE particulate film electrode

Hisao Hidaka [a,*], Tomotaka Shimura [a], Kazuhiko Ajisaka [a], Satoshi Horikoshi [a], Jincai Zhao [b], Nick Serpone [c]

[a] *Department of Chemistry, Meisei University, 2-1-1 Hodokubo, Hino, Tokyo 191, Japan*

[b] *Institute of Photographic Chemistry, Chinese Academy of Sciences, Beisatan, Beijing 100101, China*

[c] *Department of Chemistry and Biochemistry, Concordia University, 1455 deMaisonneuve Blvd. West, Montréal, (Québec), H3G 1M8 Canada*

Accepted 14 April 1997

Abstract

The photoelectrochemical degradation of amino acids and derivatives such as glutamic acid, glutamine, glutaric acid, lysine, β-alanine, 8-aminooctanoic acid and phenylalanine has been examined on an irradiated TiO_2/OTE particulate film electrode. The photooxidative disappearance of the substrates ultimately transforms the nitrogen into NO_3^- and NH_4^+ (as ammonium ions under our conditions), whereas the carbonaceous residues are converted into CO_2. Variations in photocurrent were observed during the temporal course of the photodegradative process. The rates of conversion and the quantity of degraded products depend on the external applied bias and appear to be closely related to the molecular structure of the substrates. A photoelectrochemical degradative pathway is discussed briefly on the basis of the experimental observations. © 1997 Elsevier Science S.A.

Keywords: Titanium dioxide; Semiconductor electrode; Photodegradation; Amino acids; Photocurrent; Photooxidation

1. Introduction

Illuminated aqueous titania dispersions have proven relatively effective in water purification. This notwithstanding, however, a disadvantage of such dispersions in a practical treatment process is the need to ultimately remove the TiO_2 particulates by filtration, centrifugation, coagulation and/or flocculation. Thus, any treatment process that avoids such additional costly operations will prove economically beneficial. The photodegradative oxidation of several classes of nitrogen-containing organics has already been the object of several studies by us and others [1,2]. From a biological aspect, the damage effected on an amino acid in homogeneous aqueous media by gamma radiation was reported earlier by Monig et al. [3].

A TiO_2 particulate thin film presents several interesting photochemical and photoelectrochemical properties [4–11]. Irradiation of the OTE/titania assembly by radiation equal to or greater than 3.2 eV (the bandgap for anatase titania) leads ultimately to formation of trapped electrons (e_{tr}^-; e.g. as Ti_{surf}^{III}) and trapped holes (h_{tr}^+; e.g. as $^{\bullet}OH_{surf}$) at the particle surface (Eqs. (1)–(3)):

$$TiO_2 + h\nu \rightarrow (e^-/h^+) \rightarrow e_{cb}^- + h_{vb}^+ \quad (1)$$

$$e_{cb}^- \rightarrow e_{tr}^- \quad (2)$$

$$h_{vb}^+ \rightarrow h_{tr}^+ \quad (3)$$

Application of an external bias to drive the photogenerated electrons to the counter electrode compartment in a TiO_2/OTE electrode, in which titania particles are fixed on a transparent conductive oxide glass plate, minimizes electron/hole recombination and promotes charge separation following irradiation of the assembly [6,10]. Such TiO_2/OTE electrodes exhibit photocatalytic activities that are similar to titania suspensions as observed in the photooxidative decomposition of surfactants [11] and chlorophenols [12]. They are thus preferred to suspension systems from the standpoint of removal of TiO_2 particles. This type of thin film electrode also provides a convenient method for accelerating the photocatalyzed degradation of pollutants on application of an external bias. Because of complications typically inherent in a reaction system, the mechanism(s) of the photocatalyzed mineralization of organic substances and the details of photocurrent generation in a TiO_2 particulate film electrode system have not received wide attention [13,14].

* Corresponding author.

PII S1010-6030(97)00137-8

Herein we examine the photooxidation of some amino acids and related derivatives on a TiO_2/OTE film electrode. The photodegradative process of amino acids possessing different molecular structures was monitored to provide further insights into our understanding of the photocatalytic mineralization process and on photocurrent generation.

2. Experimental

2.1. Materials

The amino acids and carboxylic acids employed, β-alanine ($NH_2CH_2CH_2COOH$), 8-aminooctanoic acid ($NH_2(CH_2)_7COOH$), glutamic acid ($HOOC(CH_2)_2C^*H(NH_2)COOH$), L-glutamine ($H_2NOC(CH_2)_2C^*H(NH_2)COOH$), L-lysine ($H_2N(CH_2)_4C^*H(NH_2)COOH$), L-phenylalanine ($C_6H_5CH_2C^*H(NH_2)COOH$) and glutaric acid ($HOOC(CH_2)_3COOH$), were all supplied by Tokyo Kasei Co. Ltd. and Ajinomoto Co. Ltd. They were used a received without further treatment. Water was bidistilled in all cases.

2.2. Methods and procedures

TiO_2 particles (Degussa P25, anatase) dispersed in an aqueous solution were loaded onto a 20×50 mm^2 fluorine-doped SnO_2 glass plate (Asahi Glass Co. Ltd.; transparent conductive oxide glass) and subsequently air-dried. The glass plate was heated to 400 °C at 1 °C min^{-1} in a furnace and then sintered for 2 h at 400 °C to obtain a particulate film electrode. The OTE coating was 2.1 μm thick, whereas the thickness of the TiO_2 thin film was 4.2 μm as measured by electron microscopic techniques. The quantity of TiO_2 particles so loaded onto a 20×30 mm^2 area of the glass plate was 5 mg. Each amino acid solution (0.1 mM, 50 ml) was contained in a two-compartment Pyrex glass photoreactor [11]. The anode electrode was the TiO_2/OTE glass plate, and the counter electrode (the cathode) was a Pt plate (20×20 mm^2); the reference electrode was an Ag/AgCl electrode connected to the assembly via a salt bridge. Applied voltages were delivered from a DC potentiostat; the UV illumination was provided by a Toshiba mercury lamp (wavelengths greater than 250 nm). The potentials at the TiO_2 electrode were measured with an electrometer. The photocurrent measurements were carried out using a potential step method with a Nikko-keisoku NPGFZ-2501A potentio/galvanostat.

2.3. Analyses

The temporal evolution of CO_2 was followed by gas chromatography with an Ookura Riken chromatograph (Model 802; TCD detection) using a Porapak Q column with helium as the carrier gas. The concentration of ammonia (as NH_4^+ ions under our conditions) was monitored with a JASCO ion chromatograph equipped with a Y-521 cationic column and with a CD-5 conductivity detector; the eluent was a nitric acid solution (4 mM). The NO_3^- ions were also monitored by ion chromatography with an I-524 anionic column using a mixed solution of phthalic acid (2.5 mM) and tris(hydroxymethyl)aminomethane (2.3 mM) as the eluent (adjusted to pH 4). The UV absorption spectra were determined on a JASCO UV-660 spectrophotometer.

The quantity of primary amine was assessed in borate buffer solution (pH 9.18) using the fluorescence emission intensity at 480 nm upon excitation of the fluorescamine/acetone mixture at 390 nm. Only a primary amine can be detected with the fluorescamine reagent (supplied by Fluka); secondary or tertiary amines are not detectable by this method [15].

3. Results and discussion

The disappearance of the primary amine and CO_2 evolution as a function of irradiation time for the photoelectrochemical oxidation of β-alanine and 8-aminooctanoic acid on the TiO_2/OTE electrode system at a constant bias of 0.5 V and at no applied potential are depicted in Fig. 1(a)–(b), respectively. As shown, the primary amine in the β-alanine structure degrades fairly rapidly within 1.5 h of irradiation under these conditions, in comparison to the case without any applied bias. A similar situation is evident in the case of the aminooctanoic acid substrate. We infer selective $^*OH$ radical (Eq.

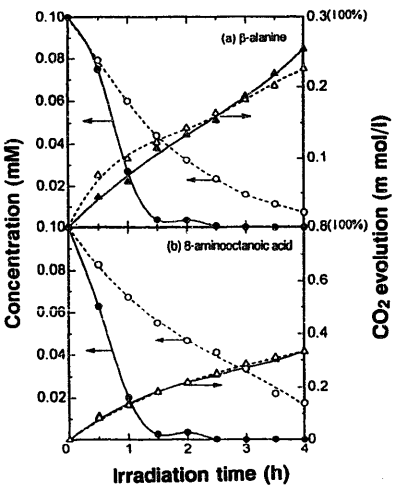

Fig. 1. Temporal behavior of the primary amine function and CO_2 evolution in the photodegradation of (a) β-alanine and (b) 8-aminooctanoic acid using an irradiated TiO_2/OTE electrode system: concentration, 0.1 mM. (●) Disappearance of the $-NH_2$ function and (▲) CO_2 evolution at constant applied potential of 0.5 V. (○) Disappearance of the $-NH_2$ function and (△) CO_2 evolution without applied bias.

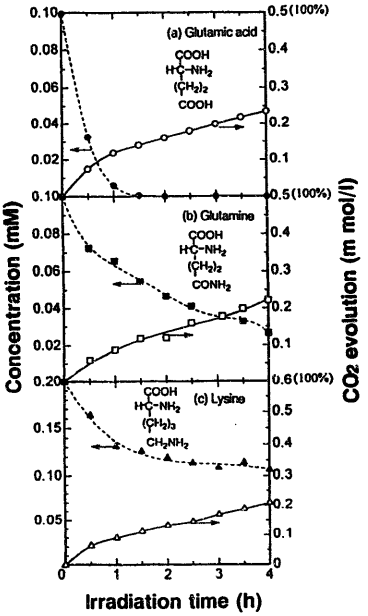

Fig. 2. Disappearance of the primary amine group and evolution of carbon dioxide versus illumination time in the photodegradation of (a) glutamic acid, (b) glutamine and (c) lysine at a constant applied bias of 0.5 V on the TiO_2/OTE electrode system: concentration, 0.1 mM. Disappearance of $-NH_2$ for (●) glutamic acid, (■) glutamine and (▲) lysine. Evolution of carbon dioxide for (○) glutamic acid, (□) glutamine and (△) lysine.

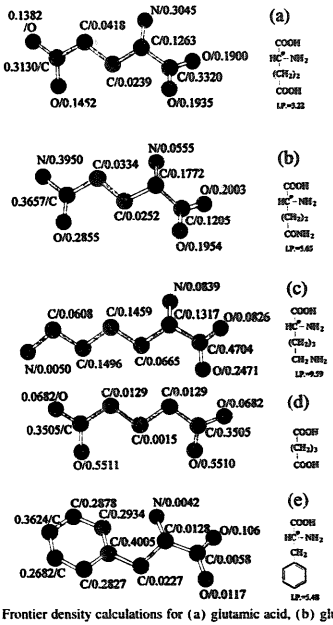

Fig. 3. Frontier density calculations for (a) glutamic acid, (b) glutamine, (c) lysine, (d) glutaric acid and (e) phenylalanine using the mopac molecular modelling program.

(3)) attack on the amine moiety; this also explains the fact that evolution of CO_2 for β-alanine is slightly suppressed under the applied bias relative to the conditions under which no bias was applied. At the culmination of the amine disappearance, evolution of carbon dioxide is relatively enhanced again.

The photodegradation of glutamic acid, glutamine and lysine and the corresponding evolution of carbon dioxide for all three substances are illustrated in Fig. 2(a)–(c), respectively. The primary amine function in glutamic acid also disappears fairly rapidly (less than 1.5 h), as seen for β-alanine, in comparison to the amine functions in glutamine and lysine, also under the applied bias. The latter two amino acids require more than 4 h of irradiation for complete degradation. The greater rate and more facile photooxidation of the primary amine functions are supported by the relatively high electron densities on the nitrogen atoms of the $-NH_2$ moiety, as shown by semi-empirical molecular orbital frontier density calculations using the mopac software (a quantum mechanical molecular modelling program) [16] and illustrated in Fig. 3(a)–(e) for glutamic acid, glutamine, lysine, glutaric acid and phenylalanine, respectively.

These mopac calculations show that the primary $-NH_2$ nitrogen in glutamic acid has a greater electron density (0.3045; Fig. 3(a)) than the corresponding nitrogens in glutamine (0.0555; Fig. 3(b)) and lysine (0.0839; Fig. 3(c)); note that for the latter structure the terminal NH_2 nitrogen has a very low electron density (0.0050). The direct oxidation by a trapped hole ($^{\bullet}OH$ radical), which scavenges the electron-rich moiety, is facilitated producing a cationic radical intermediate with the positive charge localized at the carbon bonded to the $-NH_2$ function (Eq. (4) for glutamic acid).

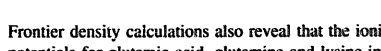

(4)

Frontier density calculations also reveal that the ionization potentials for glutamic acid, glutamine and lysine increase in the order glutamic acid (3.22 eV) < glutamine (5.65 eV) < lysine (9.59 eV) to give the corresponding radical cation species as in Eq. (4); these ionization potentials accord with the rates at which the amine function is transformed (Fig. 2). It is also worth noting that the slower rate of dis-

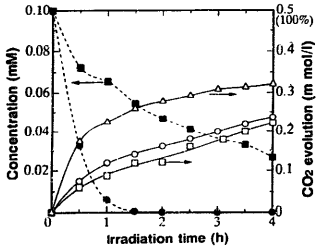

Fig. 4. Temporal behavior of the loss of the primary amine function for (●) glutamic acid and (■) glutamine, and CO_2 evolution for (○) glutamic acid, (□) glutamine and (△) glutaric acid, all at a constant applied bias of 0.5 V on an illuminated TiO_2/OTE electrode.

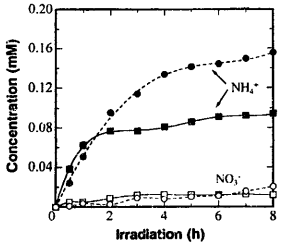

Fig. 5. Temporal formation of NH_4^+ and NO_3^- ions during the photodegradation of glutamic acid and glutamine in an irradiated TiO_2 (100 mg) aqueous suspension. NH_4^+: (■) glutamic acid and (●) glutamine. NO_3^-: (□) glutamic acid and (○) glutamine.

appearance of the primary amine in glutamine may be the result of competitive photooxidation with the amide moiety where the nitrogen has a density of 0.3950 (compare with 0.0555 for the primary $-NH_2$; Fig. 3(b)). For lysine, the adjacent primary amine to the α-carbon is more prone to attack by $^{\bullet}OH$ radicals and therefore more easily oxidized than would be the terminal primary amine for which the electron density is at least one order of magnitude smaller (0.0839 versus 0.0050, respectively; Fig. 3(c)).

In Fig. 4 we take up the temporal behavior of the disappearance of the primary amine function in glutamic acid and glutamine again for comparison and also illustrate the evolution of carbon dioxide for glutaric acid, glutamic acid and glutamine. We note that the rate of CO_2 evolution is faster for glutaric acid, followed by glutamic acid and glutamine. We expect carbon dioxide to evolve principally from attack of the carboxylate carbon by the $^{\bullet}OH$ radical to yield a radical cation and HCO_3^-, which under the usual acidic conditions used evolves into CO_2. The frontier electron density calculations of Figs. 3(a), 3(b) and 3(d) show that the density for the aliphatic carboxylate carbons in glutaric acid is larger (0.3505) than the corresponding carbons in glutamic acid (0.3320 and 0.3120) and glutamine (0.3130 and 0.1205). The electron density on the methylene carbons is at least an order of magnitude smaller.

The formation of NH_4^+ and NO_3^- ions from the photodegradation of glutamic acid and glutamine in an aqueous TiO_2 suspension system is illustrated in Fig. 5 to demonstrate the fate of nitrogen atoms in nitrogen-containing substances. We note that the primary amine functions of the amino acids are ultimately photoconverted to give greater quantities of NH_4^+ ions than NO_3^- ions after cleavage of the N–C bond.

A comparison of the photooxidative degradation of the primary amine and the phenyl moiety, together with the evolution of carbon dioxide in phenylalanine, is depicted in Fig. 6. Photoinduced conversion of the phenyl group was monitored by its UV absorption band at 208 nm. Following the disappearance of the primary amine, oxidation of the phenyl group upon attack by the $^{\bullet}OH$ radical and ultimate ring opening occur on further irradiation. Loss of the phenyl

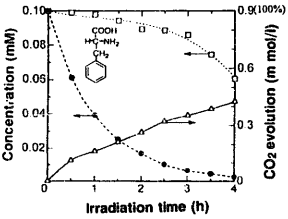

Fig. 6. Temporal loss of the primary amine group (●) and phenyl moiety (□) together with evolution of CO_2 (△) in the photodegradation of phenylalanine at a constant applied bias of 0.5 V on the TiO_2/OTE electrode system.

spectral feature (about 40% after 4 h of irradiation) at 208 nm is slow, whereas significant evolution of CO_2 takes place during the first hour of irradiation (about 17% yield). This is rather enigmatic since frontier density calculations indicate that the greatest electron density resides on the phenyl carbons.

The temporal variation of the UV spectral pattern for phenylalanine is depicted in Fig. 7. Initially, the spectra show only a feature at 208 nm. On irradiating the TiO_2/OTE/phenylalanine solution for 0.5 h, a spectral feature appears at 228 nm whose intensity increases at the expense of the 208 nm feature until 2 h of irradiation. Further illumination leads to a decrease of the 228 nm band, ascribed to absorption by a hydroxylated phenyl intermediate, and which we take to be caused by the break-up of the phenyl ring. Clearly, ring opening of the phenyl moiety is a slower process than photoconversion of the primary amine to ammonia.

Temporal variations in the photogenerated current take place during the photodegradative process for glutamic acid, glutamine and glutaric acid; they are portrayed in Fig. 8. The photocurrent increases slightly with irradiation time during the initial stages in the degradation of glutamic acid; subsequently, it decreases gradually with further illumination of the TiO_2/OTE electrode system. In the case of glutamine, the photocurrent decreases rapidly with irradiation whereas for

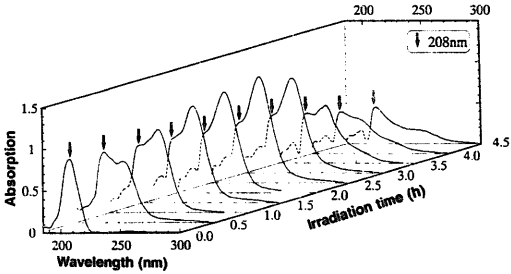

Fig. 7. UV absorption spectral profile of the temporal events taking place during the photodegradation of phenylalanine.

phenylalanine the photocurrent first decreases and then after 3 h of illumination shows a slight increase. This delayed increase in photocurrent is attributed to the photooxidation of formic acid [12], a typical principal intermediate species formed prior to CO_2 evolution as evidenced in the photodegradation of other organic compounds [12,13]. It was imperative, therefore, that we also explore the effect that the HCOOH intermediate may have on the photogenerated current during the photooxidation of the amino acids reported in this study by examining the photodegradation of formic acid.

During the initial period, a higher photocurrent was generated which decreased rapidly as formic acid degraded. In another experiment we probed the effect of the presence of formic acid on the photocurrent by adding HCOOH to the photocatalyzed degradation of 2-phenoxyethanol that had been taking place for about 2 h. The photocurrent increased dramatically upon addition of HCOOH and subsequently decreased with irradiation time. We infer that photooxidation of formic acid leads to generation of a photocurrent through the external circuit by a process described in reactions 5 and 6. Thus, subsequent to reactions 1 and 3, the trapped hole h_{tr}^+ (i.e. surface-bound $^{\bullet}OH$ radical) oxidizes formic acid to produce the $HCOO^{\bullet}$ radical (Eq. (5)) which can then inject an electron back into the TiO_2 particles and is converted to carbon dioxide (Eq. (6)).

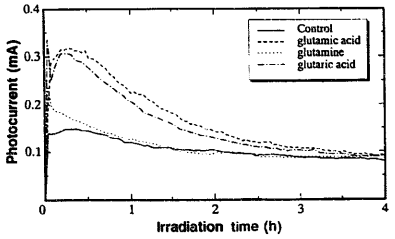

Fig. 8. Graph depicting the temporal generation of photocurrent during the photooxidative decomposition of glutamic acid, glutamine and glutaric acid (electrolyte, 0.1 M NaCl) at a constant applied bias of 0.5 V vs. Ag/AgCl.

$$h_{tr}^+ + HCOOH \rightarrow HCOO^{\bullet} + H^+ \quad (5)$$

$$HCOO^{\bullet} + TiO_2 \rightarrow CO_2 + H^+ + TiO_2(e_{tr}^-) \quad (6)$$

This is the so-called current-doubling phenomenon reported by others [14], which evidently also takes place during the photooxidation of formic acid.

Formic acid is formed in the degradation of glutamic acid by $^{\bullet}OH$ radical attack on the two carbonyl moieties during the early stages of irradiation which causes the initial increase in photocurrent. The delayed increase in the photocurrent seen after 3 h of irradiation of the phenylalanine TiO_2/OTE system is attributed to the late production of formic acid from the photooxidation of the phenyl group carbons.

4. Conclusions

Amino acids and carboxylic acids can easily be decomposed photoelectrochemically into NO_3^- and NH_4^+ ions and CO_2 on a TiO_2 particulate film electrode under an applied bias. Formation of NH_4^+ is predominant over conversion of the nitrogens in these substrates to NO_3^- ions. Application of a constant external bias enhances the photooxidative degradation of the amino acids. In a competitive degradation process between the primary amine and the phenyl moiety in phenylalanine, photocleavage of the primary amine occurs preferentially to ring opening of the phenyl group.

Acknowledgements

Our work in Tokyo is sponsored by a Grant-in-Aid for Scientific Research from the Ministry of Education (No. 06640757). The work in Beijing is partially financed by the Chinese National Science Foundation, whereas the work in Montreal is sponsored by the Natural Sciences and Engineering Research Council of Canada. We are grateful to these three agencies for their support. We also thank Asahi Glass Co. Ltd. for the kind gift of the transparent conducting oxide glass plates.

References

[1] (a) K. Nohara, H. Hidaka, E. Pelizzetti, N. Serpone, Catal. Lett. 36 (1996) 115; (b) H. Hidaka, K. Nohara, J. Zhao, E. Pelizzetti, N. Serpone, C. Guillard, P. Pichat, J. Adv. Oxid. Technol. 1 (1996) 27; (c) H. Hidaka, K. Nohara, J. Zhao, E. Pelizzetti, N. Serpone, J. Photochem. Photobiol. A: Chem. 91 (1995) 145; (d) K. Waki, L. Wang, K. Nohara, H. Hidaka, J. Mol. Catal. 95 (1995) 53; (e) H. Hidaka, K. Nohara, J. Zhao, K. Takashima, E. Pelizzetti, N. Serpone, New J. Chem. 18 (1994) 541; (f) H. Hidaka, S. Horikoshi, K. Ajisaka, J. Zhao, N. Serpone, J. Photochem. Photobiol. A: Chem., 108 (1997) 197-205.

[2] (a) G.K.-C. Low, S.R. McEvoy, R.W. Matthews, Environ. Sci. Technol. 25 (1991) 460; (b) G.K.-C. Low, S.R. McEvoy, R.W. Matthews, Chemosphere 19 (1989) 1611.

[3] J. Monig, R. Chapman, K.D. Asmus, J. Phys. Chem. 89 (1985) 3139.

[4] (a) B. O'Regan, M. Gratzel, Nature 353 (1991) 737; (b) G. Rothenberger, D. Fitzmaurice, M. Gratzel, J. Phys. Chem. 96 (1992) 5983.

[5] M.A. Anderson, Q. Xu, M. Gieselmann, J. Membr. Sci. 39 (1988) 243.

[6] Q. Xu, M.A. Anderson, J. Mater Res., 6 (1991) 1073.

[7] S. Sakohara, L.D. Tickanen, M.A. Anderson, J. Phys. Chem. 96 (1992) 11 086.

[8] (a) D. Liu, P.V. Kamat, J. Electroanal. Chem. 347 (1993) 451; (b) D. Liu, P.V. Kamat, J. Phys. Chem. 97 (1993) 10 769.

[9] S. Hotchandani, I. Bedjia, P.V. Kamat, Langmuir 13 (1994) 17.

[10] I. Bedjia, S. Hotchandani, P.V. Kamat, J. Phys. Chem. 98 (1994) 4138.

[11] (a) H. Hidaka, Y. Asai, J. Zhao, K. Nohara, E. Pelizzetti, N. Serpone, J. Phys. Chem. 99 (1995) 8244; (b) H. Hidaka, H. Nagaoka, K. Nohara, T. Shimura, S. Horikoshi, J. Zhao, N. Serpone, J. Photochem. Photobiol. A: Chem. 98 (1996) 73.

[12] (a) K. Vinodgopal, S. Hotchandani, P.V. Kamat, J. Phys. Chem. 97 (1993) 9040; (b) K. Vinodgopal, U. Stafford, K.A. Gray, P.V. Kamat, J. Phys. Chem. 98 (1994) 6797; (c) K. Vinodgopal, P.V. Kamat, Environ. Sci. Technol. 29 (1959) 941.

[13] H.O. Finklea, in: H.O. Finklea (Ed.), Semiconductor Electrodes, Elsevier, New York, 1988, pp. 1–42.

[14] (a) E.C. Dutoit, F. Cadon, W.P. Games, Ber. Bunsenges. Phys. Chem. 80 (1976) 1285. (b) Y. Maeda, A. Fujishima, K. Honda, Electrochim. Acta 128 (1981) 1731.

[15] (a) F.W. Fowler, J. Am. Chem. Soc. 94 (1972) 5977; (b) J.V. Castell, M. Cervera, R. Marco, Anal. Biochem. 379 (1979) 99.

[16] K. Nohara, H. Hidaka, E. Pelizzetti, N. Sespone, J. Photochem. Photobiol. A: Chem., 102 (1997) 279.